Biochemical and Biophysical Research Communications 425 (2012) 625–629

Contents lists available at SciVerse ScienceDirect

Biochemical and Biophysical Research Communications

journal homepage: www.elsevier.com/locate/ybbrc

Effect of enhanced Renilla luciferase and fluorescent protein variants on the Förster distance of Bioluminescence resonance energy transfer (BRET)

Helen Dacres [a,*], Michelle Michie [a], Jian Wang [a], Kevin D.G. Pfleger [b], Stephen C. Trowell [a]

[a] CSIRO Food Futures Flagship & Ecosystem Sciences, Canberra, Australia
[b] Laboratory for Molecular Endocrinology–GPCRs, Western Australian Institute for Medical Research (WAIMR) and Centre for Medical Research, The University of Western Australia, Perth, Australia

ARTICLE INFO

Article history:
Received 11 July 2012
Available online 1 August 2012

Keywords:
RLuc2
RLuc8
Venus
Coelenterazine

ABSTRACT

Bioluminescence resonance energy transfer (BRET) is an important tool for monitoring macromolecular interactions and is useful as a transduction technique for biosensor development. Förster distance (R_0), the intermolecular separation characterized by 50% of the maximum possible energy transfer, is a critical BRET parameter. R_0 provides a means of linking measured changes in BRET ratio to a physical dimension scale and allows estimation of the range of distances that can be measured by any donor–acceptor pair. The sensitivity of BRET assays has recently been improved by introduction of new BRET components, RLuc2, RLuc8 and Venus with improved quantum yields, stability and brightness. We determined R_0 for BRET^1 systems incorporating novel RLuc variants RLuc2 or RLuc8, in combination with Venus, as 5.68 or 5.55 nm respectively. These values were approximately 25% higher than the R_0 of the original BRET^1 system. R_0 for BRET^2 systems combining green fluorescent proteins (GFP^2) with RLuc2 or RLuc8 variants was 7.67 or 8.15 nm, i.e. only 2–9% greater than the original BRET^2 system despite being ~30-fold brighter.

1. Introduction

Over the last decade, Bioluminescence resonance energy transfer (BRET) has been used extensively for monitoring protein–protein interactions in living cells, particularly G-protein coupled receptor (GPCR) interactions [1,2]. More recently BRET transduction has been incorporated, with a range of biological recognition elements, into biosensors for the detection of small volatile organic molecules [3] and proteases [4–6].

BRET is a form of Förster resonance energy transfer [7] (RET) and is characterized by the non-radiative transfer of energy from a bioluminescent donor to a fluorescent acceptor. Two commonly used genetically encoded forms of BRET are BRET^1 and BRET^2, which use Renilla luciferase (RLuc) as the energy donor. In BRET^1, the substrate is coelenterazine *h* (CLZ*h*), giving peak donor emission at 475 nm and the acceptor is a yellow fluorescent protein (YFP), with a peak acceptor emission at 530 nm. There is substantial overlap between the BRET^1 donor and acceptor emission spectra resulting in a high background signal. In BRET^2, YFP is replaced with a green fluorescent protein (GFP^2) and a modified coelenterazine substrate, coelenterazine 400a (CLZ400a). The BRET^2 peak donor and acceptor emissions are shifted to 395 nm and 510 nm, respectively. This increases the separation between the donor and acceptor peaks from ~55 nm for BRET^1 to ~115 nm for BRET^2 and provides a much lower background signal [1].

Förster distance (R_0), the intermolecular distance characterized by 50% of the maximum possible energy transfer, is an informative measurement for all forms of RET. It provides a means of estimating the range of distances that can be measured by any RET probe pair. We recently experimentally determined the Förster distance of the BRET^1 and BRET^2 systems to be 4.4 and 7.5 nm respectively [8]. The longer working distance range of the BRET^2 system lends itself to the study of macromolecular rearrangements and interactions. For instance, we have shown that the BRET^2 system can be more suitable for measuring ligand-induced molecular rearrangements in GPCRs [3] compared to a FRET system with a Förster distance of 4.8 nm [8]. This is due to the experimental separation of the BRET^2 pair in this particular case being better matched to its Förster distance than the alternatives.

A major countervailing disadvantage of the BRET^2 system is that the CLZ400a substrate suffers from rapid signal decay and low quantum yield [9]. These undesirable attributes generally limit the applicability of the BRET^2 system to *in vitro* studies where measurements can be taken rapidly following substrate addition. The BRET^1 substrate has a quantum yield two orders of magnitude greater than the BRET^2 system making it more amenable, particularly to live cell and *in vivo* investigations. A BRET^2 system with a Förster distance of ~7.5 nm accompanied by a high quantum yield, or a BRET^1 system with a Förster distance similar to the BRET^2

* Corresponding author. Fax: +61 (0)2 6246 4094.
E-mail address: helen.dacres@csiro.au (H. Dacres).

0006-291X/$ - see front matter Crown Copyright © 2012 Published by Elsevier Inc. All rights reserved.
http://dx.doi.org/10.1016/j.bbrc.2012.07.133

system, would offer many advantages over the present BRET systems for biological applications. It was recently shown that the sensitivity of the BRET^2 assay can be significantly improved by substituting RLuc with novel mutant RLuc donors having improved quantum yield and stability [9,10] (Fig. 1). Venus has also been demonstrated to be a superior yellow fluorescent protein [11]. Consequently, the use of RLuc2 and RLuc8 variants with Venus for BRET^1 and GFP^2 for BRET^2 has substantially improved our ability to monitor GPCR/β-arrestin interactions in live cells using BRET [12,13]. Our aim is to determine the R_0 and consequently the useful working distance range for modified BRET^1 and BRET^2 systems incorporating RLuc2 and RLuc8 as donors to better inform choice of system. We therefore experimentally determined the variation of BRET efficiency with distance for the novel BRET^1 and BRET^2 systems.

2. Materials and methods

2.1. Assembly of BRET constructs

The BRET fusion partners RLuc2, RLuc8 and Venus were amplified and restriction cloned into a series of BRET fusion proteins containing, 1, 3, 5, 7 or 9 units of the flexible linker (FL_x) peptides $(Gly)_2Ser(Gly)_2Ser$ [8] or maltose binding protein (MBP). Standard molecular biology techniques were used with primers shown in Tables S-1 and S-2 (Supporting Information). All clones were sequenced to confirm their integrity and orientation.

2.2. Expression and purification of BRET proteins

Constructs were transformed into electrocompetent BL21 (DE3) cells (Novagen). At least three independent colonies were selected for each construct and used to perform biological replicates. Cultures were grown up and lysed using a homogeniser (Avestin emulsiflex C3 (ATA Scientific)). The BRET constructs were affinity-purified over TALON™ Superflow Metal Affinity Resin (Clontech Laboratories, Inc.) and their purity was confirmed using SDS–polyacrylamide gel electrophoresis (Fig. S-1 in Supporting Information). 1 μM purified protein was used for all BRET assays unless otherwise stated.

2.3. BRET detection

Spectral scans were recorded with a SpectraMax M2 plate-reading spectrofluorimeter (Molecular Devices). Simultaneous dual emission BRET measurements were carried out with a POLARstar OPTIMA microplate reader (BMG LabTech). BRET measurements used either the BRET^2 emission filter set comprising RLuc/CLZ400a emission filter (410 nm bandpass, 80 nm) and the GFP^2 emission filter (515 nm bandpass, 30 nm) or the BRET^1 filter set consisting of a RLuc/CLZ*h* emission filter (475 nm bandpass, 30 nm) and YFP (535 nm bandpass, 30 nm) emission filter. BRET ratios were calculated as ratios of integrated acceptor emission channel intensity to integrated donor emission channel intensity.

2.4. Förster curves

The number of flexible linker repeats was converted into distances between BRET donor and acceptor (r_{BRET}) previously [8]. Using these r_{BRET} values, Förster curves were plotted by fitting measured energy transfer efficiencies for BRET^1 ($E_{BRET}{}^1$) and BRET^2 ($E_{BRET}{}^2$) to the Förster equation (Eq. (1)) by non-linear regression.

$$E_{BRET} = \frac{R_0^6}{R_0^6 + r_{BRET}^6} \quad (1)$$

For full experimental details, see supplementary materials and methods (Supporting Information).

3. Results and discussion

3.1. Orientation

Higher BRET ratios for both BRET systems and all RLuc variants were generated when the acceptor fluorescent protein was located at the N-terminus of the fusion, and the RLuc variant at the C-terminus (Fig. 2A and B) compared with the reverse orientations. A similar orientation effect on the BRET ratio intensity was observed previously with RLuc [8]. Therefore, further studies were carried out using only fusion proteins with the orientations: Venus–FL_X–RLuc2/8 for BRET^1 studies and GFP^2–FL_X–RLuc2/8 for BRET^2 studies.

3.2. Ratiometric measurements and BRET efficiencies

BRET^1 ratios for all FL_x fusion proteins incorporating RLuc2 or RLuc8 as the donor with a Venus acceptor (Table S-3 in Supporting Information) were higher than the reported BRET^1 ratios for corresponding fusions containing RLuc and EYFP (enhanced YFP) acceptor [8]. For example, the BRET^1 ratio was previously calculated to be 3.2 ± 0.1 (S.D., n = 3) for EYFP–FL1–RLuc [8]. The BRET^1 ratios calculated here for the Venus–FL1–RLuc2 and Venus–FL1–RLuc8 fusions were 4.8 ± 0.5 (S.D., n = 6) and 5.0 ± 0.4 (S.D., n = 6), respectively. An increase in BRET^2 ratios was also observed for the BRET^2 FL_x fusion proteins with Rluc2 and RLuc8 substitutions (Table S-4 in Supporting Information) compared to the corresponding fusions incorporating RLuc [8]. Considering the dependence of energy transfer efficiency on donor quantum yield and acceptor molar absorptivity [7] it is not surprising that substitution of BRET donor

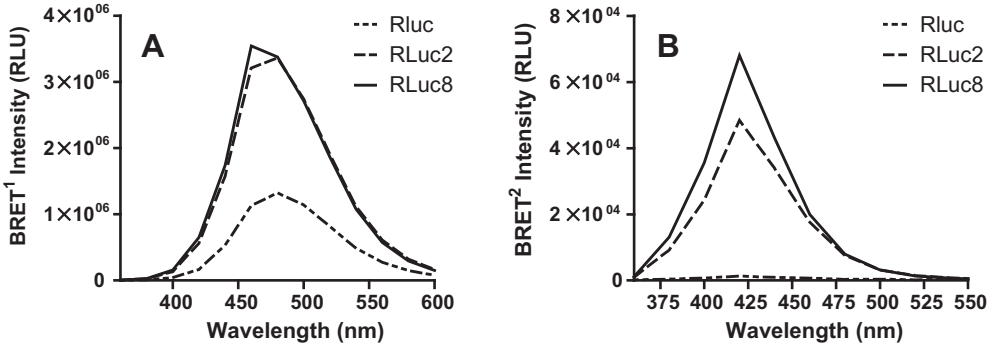

Fig. 1. Emission spectra of 1 μM purified RLuc, RLuc2 and RLuc8 upon addition of 5 μM CLZ*h* (A) and CLZ400a (B) substrate recorded with a 20 nm interval.

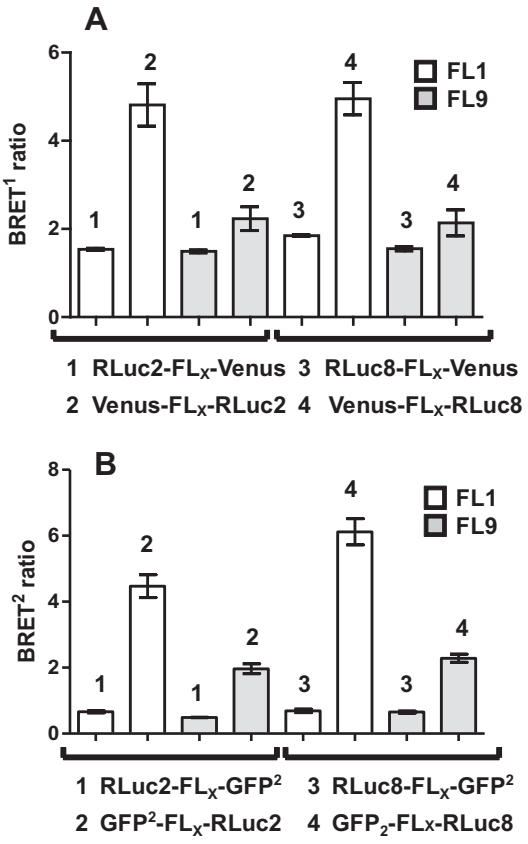

Fig. 2. Effect of orientation on BRET ratio. BRET ratios of BRET flexible linker fusion proteins (1 μM) incorporating either 1 or 9 flexible linker repeats (mean ± SD, $n = 6$) for BRET^1 fusion proteins upon addition of 5 μM CLZ*h* (A) and BRET^2 fusion proteins upon addition of 5 μM CLZ400a (B).

components with higher quantum yields and higher molar absorptivities result in higher BRET ratios.

The BRET ratios of all purified fusion proteins decreased with increasing linker length (Table S-3 and S-4, Supporting Information) due to a decrease in energy transfer efficiency with increasing separation of donor and acceptor. For determining the effect of BRET component substitutions on the measurable distance ranges of the two BRET systems we experimentally determined R_0 values to provide a direct comparison with our earlier determinations of R_0 for the original BRET systems [8]. BRET ratios (Table S-3 and S-4, Supporting Information) were converted into energy transfer efficiencies (E_{RET}) (Eq. (2)). We used the same ratiometric method (Eq. (2)) as we employed previously to calculate energy transfer efficiencies [8].

$$E_{RET} = 1 - \left(\frac{I_{DA}}{I_D}\right) \quad (2)$$

where I_{DA} is the ratio of integrated donor emission intensity to acceptor fluorescence intensity in the presence of a BRET acceptor and I_D is the ratio of donor emission intensity to acceptor fluorescence intensity in the absence of BRET [14] (see supplementary materials and methods in Supporting Information).

3.3. BRET^1 Förster curves

Fitting the data (Fig. 3) with the Förster equation (Eq. (1)) gave a R_0 of 5.68 ± 0.02 nm (mean ± SEM, $n = 6$)) for the RLuc2 and Venus BRET^1 system and 5.55 ± 0.03 nm (mean ± SEM, $n = 6$) for the RLuc8 and Venus BRET^1 system (Fig. 3A). Maltose binding protein (MBP)

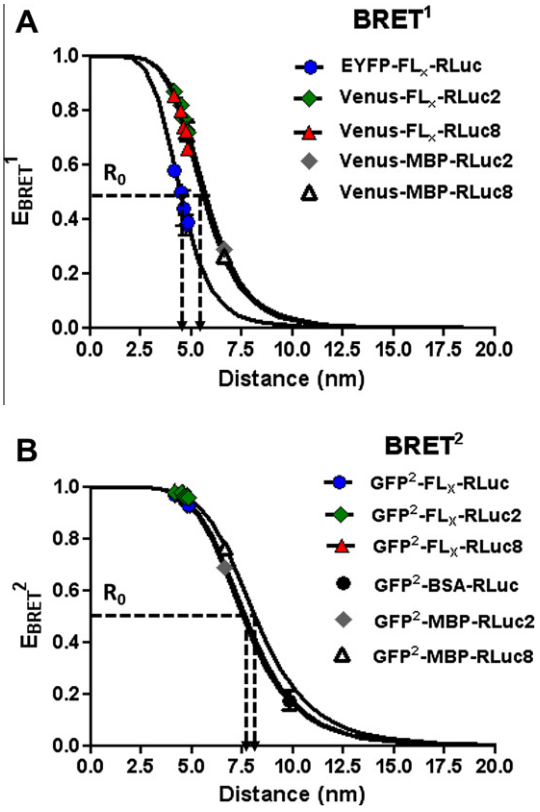

Fig. 3. Dependence of BRET efficiency on donor–acceptor separation. Experimental data are fitted with the Förster equation ($R^2 \geqslant 0.99$). Measured BRET efficiencies (E_{BRET}) of BRET^1 fusion proteins EYFP–FL$_x$–RLuc (mean ± S.D., $n = 3$), Venus–FL$_x$–RLuc2 and Venus–FL$_x$–RLuc8 (mean ± S.D., $n = 6$) (A) and BRET^2 fusion proteins GFP^2–FL$_x$–RLuc (mean ± S.D., $n = 3$), GFP^2–FL$_x$–RLuc2 and GFP^2–FL$_x$–RLuc8 (mean ± S.D., $n = 6$) (B) as a function of donor/acceptor separation (nm) (mean ± S.D., $n = 4$) [8]. The calculated E_{BRET} value (mean ± S.D., $n = 3$) for BRET^1 and BRET^2 fusion proteins separated by maltose binding protein (MBP) were plotted against the distance of 6.66 nm and the calculated $E_{BRET}{}^2$ value (mean ± S.D., $n = 5$) for GFP^2–BSA–RLuc was plotted against the distance of 9.81 nm [8].

was also inserted between the BRET^1 components (Venus–MBP–RLuc2/8). The predicted distance between the N and C terminus of MBP is 2.4 nm [15]. We previously determined [8] the radii of RLuc and GFP-like fluorescent proteins to be 2.23 nm and 2.03 nm, respectively, giving a final chromophore-to-chromophore distance of 6.66 nm. Including or excluding this data point from BRET^1 curves had no effect on the calculated Förster distance for either RLuc variant or the goodness of fit ($R^2 \geqslant 0.99$). The chromophore-to-chromophore distance between a FRET pair tagging the N and C terminus of MBP was determined to be 6.93 nm for a transfer efficiency of 0.11 and a R_0 of 4.8 nm [16]. At a transfer efficiency of 0.11 the slope of the Förster curve becomes very shallow (Fig. 3) making it difficult to accurately determine distances [17]. Using enhanced BRET^1 components the respective calculated transfer efficiencies were 0.29 and 0.26 (Table S-3, Supporting Information) for RLuc2 and RLuc8, both well within the dynamic part of the Förster curve for BRET^1 systems. Steady state RET measurements can be carried out within a range of ±50% of R_0. Outside these limits it is still possible to estimate distance but the uncertainty is increased [17]. To provide a visual comparison with the original BRET^1 Förster curve, the data points [8] for the original BRET^1 FL$_x$ fusions were also plotted (Fig. 3A). The Förster distance for the original BRET^1 system was 4.44 ± 0.03 (SEM, $n = 3$) [8]. This demonstrates that the use of brighter BRET^1 components investigated here significantly ($P < 0.001$) increased the Förster distance (from 4.44 to 5.68 nm) and shifted its useful working range from 2.20–6.66 to 2.78–8.52 nm (Fig. 4, Table S-5 in Supporting Information).

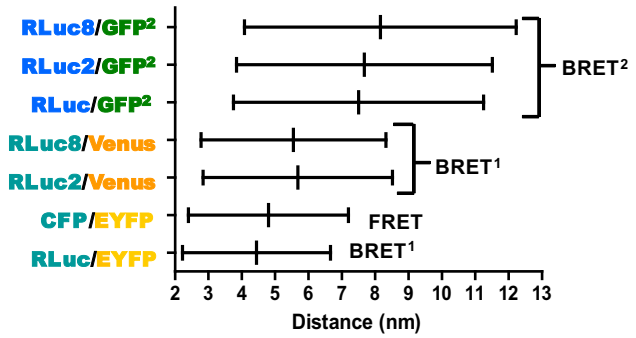

Fig. 4. Working distance range of various genetically encoded RET pairs. The distance limits are defined as ±0.5 of R_0. Vertical bars = R_0. BRET data with RLuc (RLuc/GFP^2 and RLuc/EYFP) and FRET data (CFP/EYFP) were determined in a previous paper [8].

3.4. BRET^2 Förster curves

The Förster distance of the BRET^2 system with RLuc2 as the donor is 7.67 ± 0.04 nm (mean ± SEM, n = 6) and with RLuc8 is 8.15 ± 0.02 nm (mean ± SEM, n = 6) (Fig. 3B). Non-linear regression of the Förster curve again gave an excellent fit ($R_0 \geqslant 0.99$) (Fig. 3B). BRET^2 curves with RLuc8 and RLuc are presented in Fig. S-2 (Supplementary Information). The original BRET^2 system had a Förster distance of 7.50 ± 0.03 nm (mean ± SEM, n = 3). Substitution of RLuc with either RLuc2 or RLuc8 variant increased (P = 0.03 for RLuc2 and $P \leqslant 0.0001$ for RLuc8) the Förster distance of the BRET^2 system from 7.50 to 7.67 or 8.15 nm, respectively.

3.5. Comparison of resonance energy transfer systems

The distance ranges that can be accurately measured with BRET systems using novel BRET components compared to the original BRET and FRET systems are presented in Fig. 4 (Table S-5, Supporting Information). The use of brighter BRET^1 components expands the maximum distance that the BRET^1 system can accurately measure to 8.52 nm compared with 6.66 nm for the original BRET^1 system. Substitution of the original BRET^1 components with the RLuc2 variant and Venus fluorescent protein resulted in the largest increase in the BRET^1 Förster distance from 4.44 nm to 5.68 nm. The use of RLuc 2 and 8 variants in BRET^2 further extended the maximum measurable distance range to 12.23 nm compared with 11.25 nm for the original BRET^2 system. Although the use of enhanced BRET^1 components has decreased the difference in Förster distance between BRET^1 and BRET^2 systems, all of the BRET^2 systems investigated still had larger R_0 values than any of the BRET^1 systems (Fig. 4). The RLuc8/GFP^2 BRET^2 combination has the largest Förster distance for any genetically encoded RET pair.

Using non-protein RET donor and acceptors such as near infrared (NIR) dyes, for example Cyanine 5/5.5 (R_0 = 8.3 nm), even larger distances can be measured, which could be further extended (R_0=13 nm) by the incorporation of a silver nanoparticle [18]. Although able to measure even longer distances than the enhanced BRET^2 systems described here these options require covalent coupling of the FRET fluorophores to biological macromolecules, which limits their applications. Red-shifted genetically encodable BRET components [19,20] could potentially deliver even longer range BRET for *in vivo* measurements.

RLuc variants with improved quantum yields and stability, as well as improved variants of fluorescent proteins with faster maturation times and enhanced brightness, are known to improve the sensitivity of BRET assays for live cell measurements [12,13]. Knowledge of the distance range that these BRET systems can accurately measure informs researchers on which BRET system to choose for particular applications and allows them to draw inferences about molecular scale distances. The use of brighter BRET^1 components substantially increased (~25%) the Förster distance of the BRET^1 system. We demonstrate here that the use of RLuc2 or RLuc8 BRET^2 donors enhanced signal intensity (~25-fold) but had only a marginal effect on R_0 (2–9% increase). RLuc2 and RLuc8 therefore improve the different weaknesses of both BRET systems.

Acknowledgments

The authors gratefully acknowledge Dr Murat Gel and Dr Jian-Wei Liu for advice and critical review of the manuscript. We are grateful to Sanjiv Gambhir (Stanford University, CA, USA) and Atsushi Miyawaki (RIKEN Brain Science Institute, Wako-city, Japan) for providing cDNA constructs.

Appendix A. Supplementary data

Supplementary data associated with this article can be found, in the online version, at http://dx.doi.org/10.1016/j.bbrc.2012.07.133.

References

[1] K.D.G. Pfleger, K.A. Eidne, Illuminating insights into protein-protein interactions using bioluminescence resonance energy transfer (BRET), Nature Methods 3 (2006) 165–174.
[2] K.D.G. Pfleger, R.M. Seeber, K.A. Eidne, Bioluminescence resonance energy transfer (BRET) for the real-time detection of protein-protein interactions, Nature Protocols 1 (2006) 337–345.
[3] H. Dacres, J. Wang, V. Leitch, I. Horne, A.R. Anderson, S.C. Trowell, Greatly enhanced detection of a volatile ligand at femtomolar levels using bioluminescence resonance energy transfer (BRET), Biosensors & Bioelectronics 29 (2011) 119–124.
[4] H. Dacres, M.M. Dumancic, I. Horne, S.C. Trowell, Direct comparison of fluorescence- and bioluminescence-based resonance energy transfer methods for real-time monitoring of thrombin-catalysed proteolytic cleavage, Biosensors & Bioelectronics 24 (2009) 1164–1170.
[5] H. Dacres, M.M. Dumancic, I. Horne, S.C. Trowell, Direct comparison of bioluminescence-based resonance energy transfer methods for monitoring of proteolytic cleavage, Analytical Biochemistry 385 (2009) 194–202.
[6] H. Dacres, M. Michie, S.C. Trowell, Comparison of enhanced bioluminescence energy transfer donors for protease biosensors, Analytical Biochemistry 424 (2012) 206–210.
[7] T. Förster, 10th Spiers Memorial Lecture - Transfer Mechanisms of Electronic Excitation, Discussions of the Faraday Society (1959) 7–17.
[8] H. Dacres, J. Wang, M.M. Dumancic, S.C. Trowell, Experimental determination of the Förster distance for two commonly used Bioluminescent resonance energy transfer pairs, Analytical Chemistry 82 (2010) 432–435.
[9] A. De, A.M. Loening, S.S. Gambhir, An improved bioluminescence resonance energy transfer strategy for imaging intracellular events in single cells and living subjects, Cancer Research 67 (2007) 7175–7183.
[10] A.M. Loening, T.D. Fenn, A.M. Wu, S.S. Gambhir, Consensus guided mutagenesis of Renilla luciferase yields enhanced stability and light output, Protein Engineering Design & Selection 19 (2006) 391–400.
[11] T. Nagai, K. Ibata, E.S. Park, M. Kubota, K. Mikoshiba, A. Miyawaki, A variant of yellow fluorescent protein with fast and efficient maturation for cell biological applications, Nature Biotechnology 20 (2002) 87–90.
[12] M. Kocan, H.B. See, R.M. Seeber, K.A. Eidne, K.D.G. Pfleger, Demonstration of improvements to the Bioluminescence resonance energy transfer (BRET) technology for the monitoring of G protein-coupled receptors in live cells, Journal of Biomolecular Screening 13 (2008) 888–898.
[13] M. Kocan, M. Dalrymple, R. Seeber, B. Feldman, K. Pfleger, Enhanced BRET technology for the monitoring of agonist-induced and agonist-independent interactions between GPCRs and β-arrestins, Frontiers in Endocrinology 1 (2011) 1–9.
[14] D.S. Adams, Lab Maths: A Handbook of Measurements, Calculations and Other Quantitative Skills for Use at the Bench, Cold Spring Laboratory Press, Cold Spring Harbor, New York, USA, 2003.
[15] J.A. Hall, T.E. Thorgeirsson, J. Liu, Y.-K. Shin, H. Nikaido, Two modes of ligand binding in maltose-binding Protein of Escherichia coli, Journal of Biological Chemistry 272 (1997) 17610–17614.
[16] K. Park, L.H. Lee, Y.-B. Shin, S.Y. Yi, Y.-W. Kang, D.-E. Sok, J.W. Chung, B.H. Chung, M. Kim, Detection of conformationally changed MBP using intramolecular FRET, Biochemical and Biophysical Research Communications 388 (2009) 560–564.
[17] C.G. Dos Remedios, P.D.J. Moens, Fluorescence resonance energy transfer spectroscopy is a relaible "ruler" for measuring structural changes in proteins, Journal of Structural Biology 115 (1995) 175–185.

[18] J. Zhang, Y. Fu, J.R. Lacowicz, Enhanced Förster resonance energy transfer (FRET) on a single metal particle, Journal of Physical Chemistry 111 (2007) 50–56.
[19] A. De, P. Ray, A.M. Loening, S.S. Gambhir, BRET3: a red-shifted bioluminescence resonance energy transfer (BRET)-based integrated platform for imaging protein-protein interactions from single live cells and living animals, FASEB Journal 23 (2009) 2702–2709.
[20] N. Ma, A.F. Marshall, J.H. Rao, Near-infrared light emitting luciferase via biomineralization, Journal of the American Chemical Society 132 (2010) 6884–6885.